Carbohydrate Polymers 388 (2026) 125496

Contents lists available at ScienceDirect

Carbohydrate Polymers

journal homepage: www.elsevier.com/locate/carbpol

# Development of a high-performance anion-exchange chromatography with pulsed amperometric detection based profiling approach to analyze (hetero)mannans☆

Lisa Johanna Wagner, Mirko Bunzel *

*Karlsruhe Institute of Technology (KIT), Institute of Applied Bioscience, Department of Food Chemistry and Phytochemistry, Adenauerring 20a, 76131, Karlsruhe, Germany*

ARTICLE INFO

*Keywords:*
Structural analysis
HPAEC-PAD/MS
Standard Compounds
Mannan
Mannooligosaccharides
Mannanase

ABSTRACT

Structural analysis of polysaccharides is essential for understanding their functions in the plant and their technofunctional properties in food. Therefore, a profiling approach for analyzing mannans was developed. First, enzymatically generated standard compounds representing glucomannan and galactomannan structural units were produced. Five different glucomannooligosaccharides with a degree of polymerization (DP) of 2–4 were obtained from konjac meal and four different galactomannooligosaccharides with a DP of 3–8 from locust bean gum. A combination of different liquid chromatography methods was used for their purification, followed by spectroscopic identification. Having these and additional commercially available standard compounds on hand, an analytical approach for (hetero) mannan profiling was developed and validated. This assay is based on enzymatic hydrolysis of the sample material by a specific mannanase and a semi-quantitative determination of the released oligosaccharides by high-performance anion-exchange chromatography and pulsed amperometric detection. If required, additional mass spectrometric detection can be performed. (Hetero) mannooligosaccharides released from a plant sample can thus be detected, allowing for the classification of the mannan type as demonstrated by application of the developed assay on plant materials including coffee beans, copra meal, and blackcurrant seeds.

## 1. Introduction

Mannans are hemicellulosic polysaccharides that are found in almost all plant cell walls. They consist mainly of β-1,4-linked D-mannose (Man) and can be categorized into four different structural groups: homomannans, glucomannans, galactomannans, and galactoglucomannans. Homomannans consist of β-1,4-linked Man units and are mainly found in wood and seeds. Glucomannans consist of β-1,4-linked chains of Man and D-glucose (Glc), the order of which is random (Moreira & Filho, 2008). They are common in softwood, where a Man:Glc ratio of 3:1 and a DP >200 are typical, but glucomannans are also present in hardwood with a Man:Glc ratio of 1.5–2:1 and a DP of about 70 (Van Zyl et al., 2010). A popular source of glucomannan is konjac meal (KM), which is extracted from the roots of *Amorphophallus konjac*. A Man:Glc ratio of 1.6:1 is reported for konjac glucomannans (Yao-Ling et al., 2013). Galactomannans consist of a β-1,4-linked Man backbone that carries α-1,6-linked Gal side chains. Mannans are categorized as galactomannans if their Gal content exceeds 5%, most of which are present in plants of the *Leguminosae* family (Prajapati et al., 2013). Depending on the origin of the galactomannan, both the amount and distribution of the substituents vary. Known sources of galactomannans are the seeds of the legumins guar, tara, and locust bean. Their galactomannans differ in their ratio of Man to Gal of 2:1 for guar flour, 3:1 for tara flour, and 4:1 for locust bean gum (LBG) (Moreira & Filho, 2008). The Gal side chains prevent interactions between neighboring galactomannan chains, which results in a more amorphous structure and thus increase water solubility (Van Zyl et al., 2010). The last group of mannans are the galactoglucomannans. These consist of a backbone made up of β-1,4-linked Man and Glc units, and carry α-1,6-linked Gal side chains. In addition, all mannan types can be acetylated in position *O*-2 and/or *O*-3 of the Man units (Moreira & Filho, 2008).

Mannans serve primarily as storage polysaccharides in plants,

☆ This article is part of a Special issue entitled: 'EPNOE 2025' published in Carbohydrate Polymers.

* Corresponding author.
*E-mail address:* mirko.bunzel@kit.edu (M. Bunzel).

https://doi.org/10.1016/j.carbpol.2026.125496
Received 20 February 2026; Received in revised form 22 May 2026; Accepted 27 May 2026
Available online 28 May 2026

functioning both as building block and energy reserve (Buckeridge et al., 2000; Melton et al., 2009). In addition, mannans occur in minor amounts as structural polysaccharides in the cell wall of almost all plant species (Melton et al., 2009). Examples of mannan-rich plants or plant based products that are used or produced in food industry are coffee, copra, and blackcurrants. Coffee beans are described in the literature as a typical example for the occurrence of (low substituted) galactomannans (Gniechwitz et al., 2007; Nunes & Coimbra, 2001). Copra meal is also rich in mannans and is produced in large quantities as a by-product of the production of coconut oil, fat, and milk especially in Asian countries (Cuong et al., 2024; Ghosh et al., 2015; Saittagaroon et al., 1983). In Europe, however, currants are mannan-rich plants, with large amounts of mannans, particularly found in their seeds (Hilz et al., 2005; Salo & Suomi, 1972; Steck et al., 2025).

Some mannans (e. g., galactomannans, glucomannans) form viscous solutions and are therefore used in the textile, food, paper, and pharmaceutical industries (Prajapati et al., 2013). Depending on the structure, their technofunctional properties, including viscosity, vary (Moreira & Filho, 2008; Singh et al., 2018). Therefore, an analytical approach to analyze the mannan structure is of high importance.

Several analytical methods are available for the structural characterization of carbohydrates such as the determination of the monosaccharide composition after acid hydrolysis (De Ruiter et al., 1992; Saeman et al., 1945). Other analyses offer more detailed insights into the structure of carbohydrates. For example, the methylation analysis determines the linkage positions and ring type of the monomer units (Pettolino et al., 2012; Sassaki et al., 2005). However, depending on the polysaccharide(s), there are monomers and linkage types that cannot clearly be assigned to one polysaccharide, especially in mixtures of polysaccharides. Mannans represent a group of polysaccharides that often cannot clearly be identified via these two commonly applied methods. Although in most cases Man units can be clearly assigned to mannans, this is not necessarily possible for Gal and Glc units of galacto-, gluco- and galactoglucomannans. By identification of 1,4,6-linked Man units, methylation analysis hints toward galactomannans; however, 1,4-linked Glc that occurs in glucomannans is also a monomer unit in both cellulose and xyloglucans. It is therefore necessary to develop analytical methods that support the identification of mannans and provide additional information about their structure. In the past, enzymatic-chromatographic approaches have already been successfully applied to arabinans, galactans, and xyloglucans (Steck et al., 2021; Wefers & Bunzel, 2016). These methods are based on enzymatic hydrolysis and subsequent detection of the oligosaccharides using high-performance anion-exchange chromatography (HPAEC) with pulsed amperometric detection (PAD). Polysaccharides are selectively cleaved into oligosaccharides using a specific enzyme. These oligomeric building blocks can subsequently be identified and quantified using standard compounds and relative response factors (RRF).

The aim of this study was to develop a profiling approach to analyze the structures of mannans. Thus, non-commercially available gluco- (GlcMOS) and galactomannooligosaccharides (GalMOS) were isolated as standard compounds. Using these standard compounds, a chromatographic method for the semi-quantitative determination of mannans was developed and applied to various plant based samples. We hypothesize that the developed approach based on enzymatic hydrolysis detects enzyme accessible mannan regions, thus providing us with valuable information about the nature of the (galacto-/gluco-)mannnans in plants of specific botanical families and genera. However, highly substituted or crystalline areas are unlikely to be efficiently hydrolyzed as is known from previous enzyme based profiling approaches for plant based polysaccharides. Despite this limitation, we aim to develop a rapid screening of mannan structural characteristics in plant samples using standard carbohydrate analysis technique such as HPAEC-PAD that is transferable to other laboratories.

## 2. Materials and methods

### 2.1. Materials and reagents

For the isolation of standard compounds, LBG from Carl Roth (Karlsruhe, Germany) and KM from Buxtrade (Buxtehude, Germany) were used. Additional samples of LBG were from Natura (Hannover, Germany), Idda Herbal (Sofia, Bulgaria), and Alpi Nature (Sofia, Bulgaria); samples of KM were from RheinNatur (Kempen, Germany), Vita2You (Furth, Germany), and Mynatura (Hünxe, Germany). Plant samples were purchased from local grocery stores. Mannobiose ($Man_2$), mannotriose ($Man_3$), mannotetraose ($Man_4$), mannoheptaose ($Man_5$), mannohexaose ($Man_6$), and a specific *endo*-β-1,4-mannanase ($MAN_S$, from *Aspergillus niger*, EC 3.2.1.78, ~600 U/mL) were purchased from Megazyme (Bray, Ireland). An additional mannanase produced for industrial purposes ($MAN_I$, produced by *Trichoderma reesei*, EC 3.2.1.78) was provided by the producer. Thermostable α-amylase Termamyl 120 L (≥500 U/mg protein (biuret), from *Bacillus licheniformis*, EC 3.2.1.1), amyloglucosidase (≥260 U/mL, from *Aspergillus niger*, EC 3.2.1.3), protease Alcalase 2.4 L (2.4 U/g, from *Bacillus licheniformis*, EC 3.4.21.62), sodium dihydrogen phosphate, and disodium hydrogen phosphate from Sigma-Aldrich (St. Louis, Missouri, USA) were used for preparative isolation of dietary fiber fractions. Also, acetanilide, 2-deoxy-D-Glc, monosaccharide standard compounds (Man, Glc, Gal, galacturonic acid, glucuronic acid, xylose, fucose, arabinose, rhamnose), isomaltotriose (IMT), lithium chloride, methanolic hydrochloric acid, sodium acetate, sulfuric acid, and trifluoroacetic acid (TFA) were from Sigma-Aldrich (St. Louis, Missouri, USA). Ethanol, acetonitrile, sodium hydroxide (NaOH), and sodium acetate were purchased from VWR (Radnor, Pennsylvania, USA) and deuterium oxide from Deutero (Kastellaun, Germany).

### 2.2. Preparation of standard compounds

#### 2.2.1. Enzymatic hydrolysis of mannans

Standard compounds of GlcMOS and GalMOS were obtained by enzymatic hydrolysis using mannanase and a gluco- or galactomannan-rich raw material. To release GlcMOS from KM, 1 g of KM was dissolved in 1 L of deionized water. After adding 10 μL of $MAN_S$, the solution was incubated for 48 h at 60 °C with shaking. For GalMOS, 10 g of LBG was dissolved in 1 L of deionized water, and 100 μL of $MAN_S$ or 10 mg of $MAN_I$ was added. The solution was incubated for 48 h at 60 °C ($MAN_S$) or 50 °C ($MAN_I$) while shaking. The two different mannanases resulted in different release patterns, which simplified the isolation of certain GalMOS. After incubation, the mannanase was inactivated at 95 °C for 10 min. Four volumes of ethanol were added to the solution (final ethanol concentration: ca. 80% (*v*/v)) to precipitate residual polysaccharides, followed by centrifugation, and the supernatant was evaporated.

#### 2.2.2. Separation with size exclusion chromatography

The GlcMOS and GalMOS mixtures were separated by size exclusion chromatography (SEC) using a column packed with Bio Gel P-2 (bed volume: 85 × 2.6 cm, Bio-Rad Laboratories, Feldkirchen, Germany) at 45 °C and portions of around 250 mg of the GlcMOS mixture or 2 g of the GalMOS mixture, respectively. The eluent was deionized water (flow rate: 0.5 mL/min). A Smartline refractive index (RI) detector 2300 (Knauer, Berlin, Germany) was used for detection. Fractions of the eluate (Fig. S 1) were collected 6 min each and combined according to the elution profile.

#### 2.2.3. Purification of gluco- and galactomannooligosaccharides

For further purification, selected SEC fractions were separated using a high-performance liquid chromatography (HPLC) system (Azura P2.1L, Knauer, Berlin, Germany) with a porous graphitic carbon (PGC) column (Hypercarb, 5 μm particle size, 100 × 4.6 mm, Thermo Fisher

Scientific, Waltham, Massachusetts, USA) and/or an HPAEC system (Thermo Fisher Scientific, Waltham, Massachusetts, USA) with a CarboPac PA-100 column (8.5 μm particle size, 250 × 9 mm, Thermo Fisher Scientific, Waltham, Massachusetts, USA). Eluents for PGC-HPLC were double deionized water and acetonitrile; the gradients were chosen according to the SEC fraction to be separated. The column temperature was 70 °C and the flow rate 1 mL/min. The eluate was split (ratio 1:20), and the smaller part was detected by evaporative light scattering detection (ELSD, Sedex 85, ERC GmbH, Riemerling, Germany, 40 °C), whereas the larger part was collected according to the elution profile by using a programmable multiposition valve (Azura V2.1S, Knauer, Berlin, Germany). HPAEC was run with double deionized water, 0.1 M NaOH, and 0.1 M NaOH +0.5 M sodium acetate as eluents (flow rate: 2 mL/min, column temperature: 25 °C). Samples were manually injected, and the elution profile was monitored by PAD (Dionex ICS-5000 DC, Thermo Fisher Scientific, Waltham, Massachusetts, USA). Again, the eluate was split (ratio 1:15) and directed to the detector and the fractionation valve, respectively (UltiMate AFC-3000, Thermo Fisher Scientific, Waltham, Massachusetts, USA). The collected fractions were neutralized with 0.1 M HCl and desalted by nonporous graphitic carbon solid phase extraction (nPGC-SPE, 250 mg, 3 mL, Supelclean ENVI-Carb, Sigma-Aldrich, St. Louis, Missouri, USA). The nPGC-SPE was conditioned with acetonitrile (3 × 1 mL) and double deionized water (3 × 1 mL), washed with double deionized water (4 × 1 mL), and oligosaccharides were eluted using an acetonitrile:double-deionized water mixture r (50:50, 3 × 1 mL). After HPLC or HPAEC/nPGC-SPE, the eluates, were evaporated to remove acetonitrile and freeze-dried.

#### 2.2.4. Structural elucidation of standard compounds

To elucidate the structures of the isolated standard compounds, the monosaccharide composition and the degree of polymerization (DP) were determined. Furthermore, $^{1}$H and two-dimensional (2D) nuclear magnetic resonance (NMR) spectroscopy were performed.

The monosaccharide composition was investigated following TFA hydrolysis and HPAEC-PAD. The isolated compounds were treated with TFA (2 M for 1 h at 121 °C) to cleave the glycosidic bonds (Albersheim et al., 1967). TFA was evaporated and the samples were co-evaporated twice with ethanol to remove acid traces. The residues were dissolved in double deionized water, and 2-deoxy-D-Glc (final concentration: 25 μM) was added as internal standard. The samples were analyzed with HPAEC-PAD using a CarboPac PA-20 column (6 μm particle size, 150 × 3 mm, Thermo Fisher Scientific, Waltham, Massachusetts, USA) at 25 °C and double deionized water (A), 0.1 M NaOH (B), and 0.1 M NaOH +0.5 M sodium acetate (C) as mobile phase (flow rate: 0.4 mL/min). Prior to injection, the column was rinsed with 100% B for 10 min and with 90% A and 10% B for 10 min. The eluent composition was linearly changed from 0 to 1.5 min to 97% A and 3% B, followed by an isocratic elution from 1.5 to 22 min, and a linear change from 22 to 27 min to 100% B. The last 10 min of elution were performed isocratically with 60% B and 40% C. For calibration, Man, Glc, and Gal standards were used in concentrations of 1–125 μM. The monosaccharide composition of the isolated standard compounds was analyzed in duplicate.

To obtain information about the purity and DP of the isolated compounds, they were analyzed by HPAEC-PAD coupled with an electrospray (ESI) single quadrupole mass spectrometric detector (MS) (Thermo Fisher Scientific, Waltham, Massachusetts, USA). An HPAEC system (Thermo Fisher Scientific, Waltham, Massachusetts, USA) with a CarboPac PA-200 column (6 μm particle size, 250 × 3 mm, Thermo Fisher Scientific, Waltham, Massachusetts, USA) at 25 °C and double deionized water, 0.1 M NaOH, and 0.1 M NaOH +0.5 M sodium acetate as mobile phase (flow rate: 0.4 mL/min) was used. Individually adapted gradients were used for each standard compound. For the simultaneous detection by PAD and MS, the eluate was split and the part directed toward MS was desalted by an electrolytically regenerated suppressor (Dionex AERS 500 + AXP pump, Thermo Fisher Scientific, Waltham, Massachusetts, USA). The desalted eluate was continuously monitored by a conductivity detector (Thermo Fisher Scientific, Waltham, Massachusetts, USA). In order to create stable adducts in the ESI positive mode, LiCl was added to the eluate via a T-fitting and an additional pump (Dionex AXP-MS, Thermo Fisher Scientific, Waltham, Massachusetts, USA) before reaching the MS ion source. The formed Li adducts of the analyte were detected as $[M + Li]^{+}$ or $[M + 2Li]^{2+}$. The mass to charge ratios ($m/z$) of these quasi molecular ions were used to calculate the DP. The purity of the standard compounds was estimated using PAD peak area ratios of the analyte peak compared to the sum of additional peaks in the chromatogram without using corrections factors.

Structural details were obtained from NMR spectroscopic experiments using a Bruker Ascend 500 MHz spectrometer (Bruker Corporation, Rheinstetten, Germany) equipped with a Prodigy cryoprobe operated at 298 K. Standard Bruker pulse sequences were employed for $^{1}$H (zg30), HSQC (hsqcedetgp), HSQC-TOCSY (hsqcetgpml), HMBC (hmbcgplpndqf), and H2BC (h2bcetgpl3) experiments. To reduce acquisition time, nonuniform sampling with a sampling density of 50% was applied for all 2D experiments. The isolated standard compounds were solubilized in deuterium oxide, and the signals were referenced against acetone ($\delta_H = 2.22/\delta_C = 30.89$ ppm).

#### 2.2.5. Method setup: quantification of standard compounds, chromatographic conditions, and determination of relative response factors

To obtain stock solutions with a defined concentration, the isolated GlcMOS and GalMOS standard substances (Fig. 2) were measured by quantitative $^{1}$H NMR using the internal standard compound (ISTD) acetanilide ($\delta$ = 2,17 ppm) and applying a D1 relaxation delay of 15 s. Due to the direct proportionality between the intensity of the signal and the number of nuclei, it is possible to determine the concentration of the solubilized compounds via the ratios of peak areas of selected signals of the analyte and the ISTD. The signals of the anomeric protons (α- + β-anomer) are suitable for GlcMOS and GalMOS because of a good separation from other signals. Based on the concentrations determined, 1 mM stock solutions were prepared and used for further method development.

By using both the commercially available and the isolated standard compounds, the HPAEC-PAD method was developed. The final method was performed on a CarboPac PA-200 column (6 μm particle size, 250 × 3 mm, Thermo Fisher Scientific, Waltham, Massachusetts, USA) at 25 °C and double deionized water (A), 0.1 M NaOH (B), and 0.1 M NaOH +0.5 M sodium acetate (C) were used as mobile phase (flow rate: 0.4 mL/min). The gradient program was as follows: 100% C for 10 min followed by 90% A and 10% B for 20 min in order to equilibrate the column. After injection of 25 μL of the aqueous sample solution, elution was performed for 45 min using 90% A and 10% B. Until 55 min, the gradient was changed linearly to 45% A and 55% B and until 80 min to 20% A and 80% B. To clean the column, it was rinsed using 100% C for 10 min. Using this gradient program, coelution occurs only for $Man_5$ and $Gal^{3}Man_3$. To distinguish between these two analytes and to determine the peak area ratio of $Man_5$ and $Gal^{3}Man_3$, the sample can be re-run with a second elution program. The second elution program started with 100% C for 10 min and 90% A and 10% B for 20 min (equilibration). After injection of 25 μL of the sample, elution was performed with 95% A and 5% B for 45 min. To clean the column, it was rinsed with 100% C for 10 min.

Calibration curves were used for the semi-quantitative determination of the analytes. These were set up for all MOS (Man to $Man_6$), GalMOS, and GlcMOS (Fig. 2) contained in the method using individually defined calibration ranges. The linear adjustment using IMT as ISTD enabled the determination of relative response factors (RRF). Thus, it is not necessary to perform a new calibration for each series of measurements, saving valuable standard compounds. To enable quantification via RRF and peak areas (PA), the calibration curves must be set up according to the following equation and forced through the origin: c(analyte) = RRF * c(IMT) * PA(analyte)/PA(IMT). RRF corresponds to the slope of the curve. The method was validated by measuring the calibration curves

with IMT (final concentration: 10 μM) in triplicate and calculating the following statistical parameters: correlation coefficients, process coefficients of variation (ratio of standard deviation of the procedure to the center of the calibration range), limit of detection (LOD), and limit of quantification (LOQ). The latter two were determined by estimating the signal-to-noise ratio with LOD ≥3:1 and LOQ ≥9:1.

### 2.3. Application of the approach

#### 2.3.1. Isolation of dietary fiber

Isolation of insoluble (IDF) and soluble dietary fiber (SDF) was carried out according to the method described by Bunzel et al. (2001). In brief, 10 g of the milled sample (particle size <0.5 mm) was solubilized in 100 mL of sodium phosphate buffer (0.08 M, pH 6.0). To degrade starch and proteins, the sample was incubated with thermostable α-amylase (Termamyl 120 L, Sigma-Aldrich) for 20 min at 92 °C, followed by protease (Alcalase 2.4 L, Sigma) for 30 min at 60 °C and pH 7.5, and amyloglucosidase (≥260 U/mL, Sigma-Aldrich) for 30 min at 60 °C and pH 4.5. To separate IDF and SDF, the sample solution was centrifuged, and the supernatant was separated and stored; IDF remained as residue. The supernatant was precipitated by adding 4 times the volume of ethanol. After centrifugation, SDF was obtained as residue. Analysis of KM and LBG did not require fiber isolation due to the high mannan content of these samples.

#### 2.3.2. Monosaccharide composition of the isolated fiber fractions

The determination of the monosaccharide composition of IDF and SDF provides helpful information about the occurrence of mannans without a detailed analysis of the mannan structure. Hydrolysis of IDF was performed using sulfuric acid (12 M for 30 min under cool conditions and for 2 h at room temperature, then 1 M for 3 h at 100 °C) to capture crystalline polysaccharide regions (Saeman et al., 1945). The hydrolyzed samples were neutralized with NaOH and filtered. SDF samples were treated with methanolic hydrochloric acid (1.25 M for 16 h at 80 °C) followed by TFA (2 M for 1 h at 121 °C) (De Ruiter et al., 1992). The hydrolyzed samples were evaporated and co-evaporated twice with ethanol to remove TFA residues. All samples were dissolved or diluted in/with double deionized water, and 2-deoxy-D-glucose (final concentration: 25 μM) was added as internal standard. The samples were analyzed as described in 2.2.4. For calibration, standards of Man, Glc, and Gal, arabinose, xylose, fucose, rhamnose, galacturonic acid, and glucuronic acid were used in concentrations of 1–125 μM. IDF and SDF samples were analyzed in duplicate.

#### 2.3.3. Application of the mannan profiling approach

Sample material (e.g., IDF, SDF; 10 mg) was dissolved/suspended in 500 μL of double deionized water. $MAN_S$ (1 μL) was added and the sample was incubated for 24 h at 60 °C. After that, the sample was treated for 10 min at 95 °C to inactivate the mannanase, and the sample was centrifuged. The supernatant was diluted, IMT was added (final concentration: 10 μM IMT), and the sample was analyzed by HPAEC-PAD (optional coupled with MS) as described in Section 2.2.5. All samples were analyzed in duplicate and in comparison to a control sample, which was treated as described but without the addition of mannanase.

#### 2.3.4. Size exclusion chromatography of polymeric and hydrolyzed sample parts

Both the still polymeric and the hydrolyzed part of a mannanase treated sample were analyzed by high-performance size exclusion chromatography (HPSEC, LaChrome, Hitachi, Merck, Darmstadt, Germany) with refractive index detection (Smartline RI detector 2300; Knauer, Berlin, Germany). As stationary phase two columns (Tosoh TSKgel G6000 PWxl and Tosoh TSKgel G4000 PWxl, 12 μm particle size, 40 × 6.0 mm, Tosoh Bioscience, Tokyo, Japan) were coupled in a row. The mobile phase was double deionized water (flow rate: 0.5 mL/min) at 50 °C. The eluate was collected manually according to its elution profile. Collected samples were freeze-dried and analyzed for their monosaccharide composition after acidic hydrolysis as described in Section 2.3.2 for SDF.

## 3. Results and discussion

### 3.1. Generation and structural elucidation of gluco- and galactomannooligosaccharide standard compounds

#### 3.1.1. Isolation of standard compounds

Only unsubstituted MOS with a DP of 1–6 were commercially available for the development of a profiling approach to analyze mannans following enzymatic hydrolysis. Therefore, the isolation and identification of GlcMOS and GalMOS was necessary. Incubation of KM with an *endo*-β-1,4-mannanase was performed to release GlcMOS. By comparison with MOS standard substances and interpretation of MS data (HPAEC-PAD/MS), five signals were suspected to be GlcMOS and selected for further isolation (Fig. 1a). Their Li-adducts reveal a DP of 2 (*m/z* 349), 3 (*m/z* 511), and 4 (*m/z* 673). Changing the incubation conditions did not result in a significant change in the release pattern. Enzymatic hydrolysis products described in the literature are predominantly mono-, di- and trisaccharides, too (Cescutti et al., 2002; Mikkelson et al., 2013).

To release GalMOS, LBG was treated with two different *endo*-β-1,4-mannanases (Fig. 1b). Analysis of the hydrolysates revealed different release patterns with different dominant oligosaccharides, simplifying the isolation of potential standard compounds. However, both enzymatic treatments preferentially released mannobiose and mannose, in case of $MAN_S$ additionally mannotriose. Comparison of additional signals with those of MOS standard compounds and interpretation of MS data (quasi-molecular ions of the Li-adducts) suggested that the additional signals represent GalMOS. Four GalMOS with DP of 3 (*m/z* 511), 4 (*m/z* 673), 7 (*m/z* 583), and 8 (*m/z* 664) - the latter two *m/z* represent the adducts containing two Li ions - were selected for further isolation.

After enzymatic treatment, remaining polysaccharides were precipitated using 4 volumes of ethanol to reach ca. 80% ethanol (*v*/v). This additional step made it possible to achieve a good separation using preparative SEC. Good separation according to DP was achieved, especially for smaller (Gal/Glc)MOS up to a DP of 4. With increasing molecular size, however, the separation according to DP became worse, but the fractions obtained were still suitable for further isolation. Further purification steps included PGC-HPLC and/or HPAEC to isolate all nine selected GalMOS and GlcMOS in a desired purity of >90%. Although HPAEC is a routine method for analyzing carbohydrates (Cataldi et al., 2000; Corradini et al., 2012; Lee, 1990), semipreparative fractionation using HPAEC is not yet widely used. Due to the necessary neutralization and desalting steps of the isolated fractions, HPAEC fractionation requires further workup steps but offers an additional separation mechanism to obtain oligosaccharides that are otherwise difficult to separate.

#### 3.1.2. Structural characterization of standard compounds

After identification (see below), the isolated oligosaccharides (Fig. 2) were named according to the following nomenclature. Each unsubstituted Man unit is indicated as 'Man'; if there are more than one unit the number of Man units is indicated by a subscript number. The same procedure is used for backbone Glc units (for example '$GlcMan_2$'); the non-reducing sugar is written left, the reducing sugar on the right. The number of substitutions with Gal units and the localization within the mannose-based backbone (indicated by superscript letters) are found at the beginning of the label with the position being counted from the non-reducing end (for example '$Gal^2Man_2$'). Naming is always from the terminal end to the reducing end. An overview of the structures and names of the isolated oligosaccharides is shown in Fig. 2.

For structural elucidation, the monosaccharide composition following hydrolysis and the DP (via MS data) of the isolated compounds

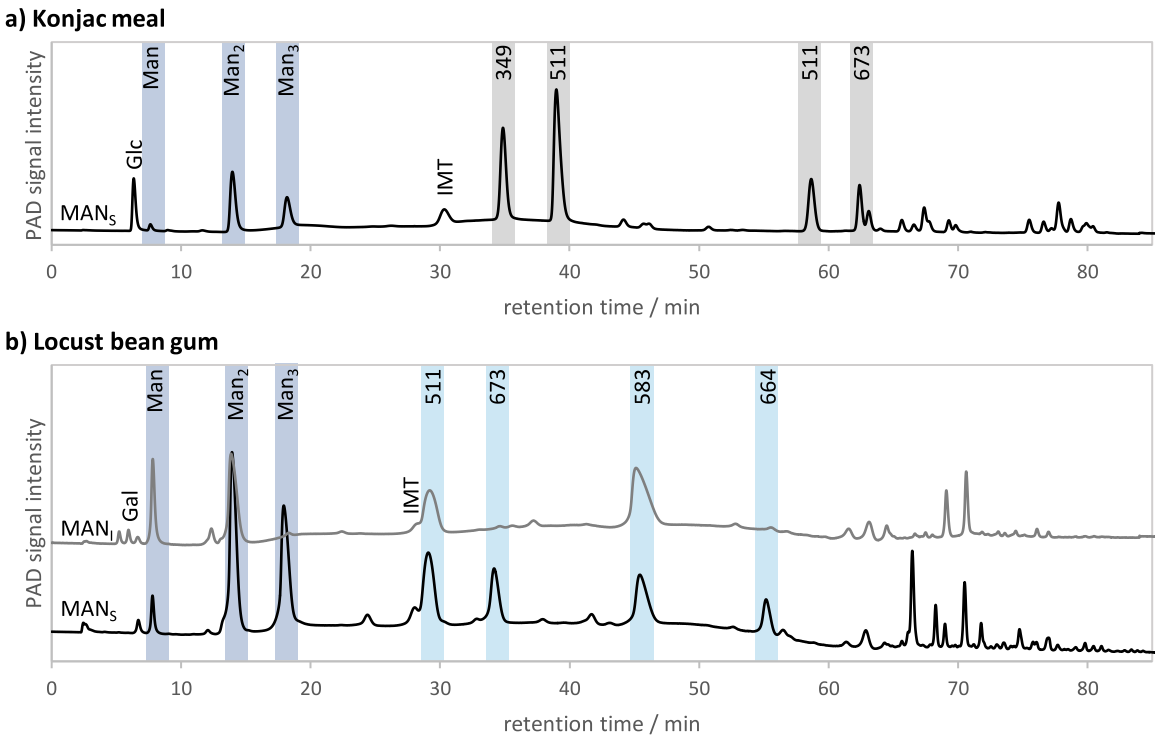


**Fig. 1.** Chromatograms of the hydrolysates of a) konjac meal with a specific *endo*-β-1,4-mannanase ($MAN_S$) and b) locust bean gum with $MAN_S$ and an industrially manufactured mannanase ($MAN_I$), analyzed by high-performance anion-exchange chromatography with pulsed amperometric detection (PAD). Mannooligosaccharides (dark blue) and gluco- (gray) and galactomannooligosaccharides (light blue) selected for further isolation are highlighted. The numbers describe the mass-to-charge ratios of the single or double charged Li-adducts of the corresponding signals. A method was later developed that resolved the peaks (Fig. 3). Man: mannose, $Man_2$: mannobiose, $Man_3$: mannotriose, Glc: glucose, Gal: galactose, IMT: isomaltotriose.

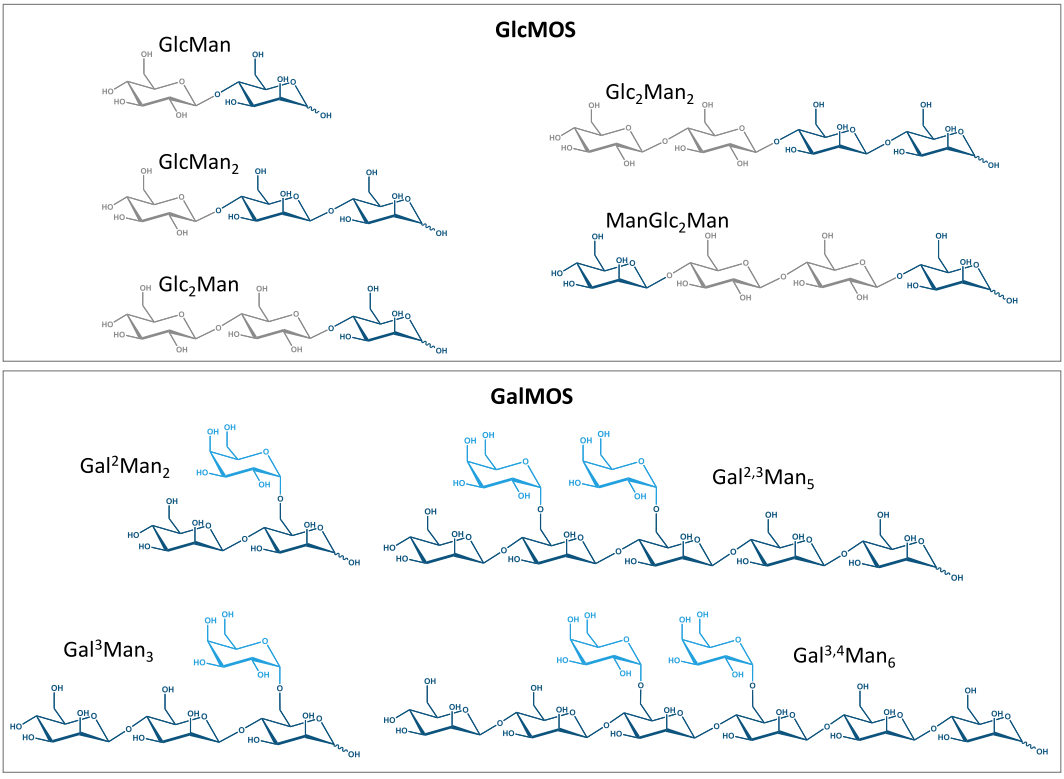


**Fig. 2.** Structures of the isolated gluco- and galactomannooligosaccharides.

were determined. Concerning the GlcMOS, a disaccharide, two trisaccharides, and two tetrasaccharides were isolated with Man:Glc

ratios of 1:1, 2:1, 1:2, and 2:2, respectively. The four isolated GalMOS from LBG were tri-, tetra, hepta- and octasaccharides with Man:Gal ratios of 2:1, 3:1, 5:2, and 6:2, respectively. The level of substitution of the GalMOS fits well with the degree of substitution of LBG, which is typically 25% (Moreira & Filho, 2008; Prajapati et al., 2013).

To determine glycosidic linkages and monomer configurations, $^{1}$H NMR and various 2D NMR experiments were performed. $^{1}$H NMR spectra, providing initial information about the structure of the GlcMOS and GalMOS, are shown in Fig. S 2. Typical signals and signal regions of MOS can already be identified based on comparison with data from mannotriose (Fig. S 2a): The signals with the largest chemical shift (downfield doublets) represent anomeric protons. Based on the coupling constants, the signal at 5.17 ppm is assigned to *H*-1 of the α-anomer ($^{3}J_{H,H}$ = 1.39 Hz) and the signal at 4.91 ppm to *H*-1 of the β-anomer ($^{3}J_{H,H}$ = 0.75 Hz), each representing the reducing Man unit. Comparable coupling constants (α-anomer: $^{3}J_{H,H}$ = 1.6 Hz, β-anomer: $^{3}J_{H,H}$ = 0.8 Hz) were described in literature (Bubb, 2003). In all isolated oligosaccharides, the signals of the α- and β-anomer protons of the reducing unit show similar chemical shifts, suggesting a reducing Man unit in all isolated oligosaccharides. Furthermore, GlcMOS and GalMOS can already be distinguished using $^{1}$H NMR. All GlcMOS exhibit *H*-1 signals of the Glc unit(s) in the range from 4.48 to 4.53 ppm. The *H*-1 signal of the Glc unit of GlcMan occurs as two doublets due to long-range effects of the reducing Man unit, which is present in an equilibrium of α- and β-pyranose (Cescutti et al., 2002). Based on the *H*-1 coupling constants ($^{3}J_{H,H}$ ≈ 7.95 Hz) Glc is always in its β-configuration (Karplus, 1959). For GalMOS, characteristic *H*-1 signals in the range of 5.00 to 5.04 ppm were assigned to Gal unit(s). Based on the *H*-1 coupling constant of approximately 4 Hz, Gal is present in its α-configuration (Duus et al., 2000). The *H*-1 signals of terminal and mid-chain Man units are found in the range from 4.74 to 4.76 ppm but are partially superimposed by the signal of residual water. The signal of the remaining ring protons (*H*-2–*H*-6) are in the range of 3.40 to 4.20 ppm.

2D NMR was primarily used to determine the positions of Glc and Gal units in GlcMOS and GalMOS. After assigning the *C*-1/*H*-1 to *C*-6/*H*-6 signals to the monomer units using the HSQC, HSQC-TOCSY, and H2BC spectra (for chemical shifts Table S 1–Table S 9), the linkages between the monomers were determined by interpretation of the HMBC spectrum. Cross signals showing the coupling of protons and $^{13}$C via three bonds reveal the position of glycosidic bonds. For example, for GlcMan$_2$ two cross signals ($\delta_H$ = 4.49/$\delta_C$ = 77.29 ppm and $\delta_H$ = 3.78/$\delta_C$ = 103.35 ppm) were detected between the *C*-1/*H*-1 signal of the Glc unit ($\delta_H$ = 4.48/$\delta_C$ = 103.39 ppm) and the *C*-4/*H*-4 signal of the non-reducing Man unit that is positioned in the middle ($\delta_H$ = 3.77/$\delta_C$ = 77.30 ppm) as well as two cross signals ($\delta_H$ = 4.76/$\delta_C$ = 77.46 ppm and $\delta_H$ = 3.90/$\delta_C$ = 100.61 ppm) between the *C*-1/*H*-1 signal of this non-reducing, middle-position Man unit ($\delta_H$ = 4.76/$\delta_C$ = 100.65 ppm) and the *C*-4/*H*-4 signal of the reducing Man unit ($\delta_H$ = 3.90/$\delta_C$ = 77.45 ppm), revealing the structure shown in Fig. 2. The position of the Gal units in GalMOS was also localized by interpretation of the HMBC spectra. In case of Gal$^{2}$Man$_2$, a cross signal ($\delta_H$ = 5.01/$\delta_C$ = 67.27 ppm) was detected between the *C*-1/*H*-1 signal of the Gal unit ($\delta_H$ = 5.01/$\delta_C$ = 99.44 ppm) and the *C*-6/*H*-6 signal of the reducing Man unit ($\delta_H$ = 4.01/$\delta_C$ = 67.30 ppm and $\delta_H$ = 3.71/$\delta_C$ = 67.30 ppm), thus, demonstrating that Gal is linked to the reducing Man unit. Accordingly, interpretation of the 2D NMR spectra allowed for an unambiguous identification of all isolated GlcMOS and GalMOS (Fig. 2) in accordance with (Cescutti et al., 2002; Mccleary & Matheson, 1983; Mikkelson et al., 2013).

### 3.2. Development of a profiling approach and its evaluation

#### 3.2.1. Standard solutions, chromatographic conditions, and determination of relative response factors

An HPAEC based separation of almost all GlcMOS, GalMOS, and MOS standard compounds and the internal standard IMT was established (Fig. 3). Only the separation of mannopentaose and Gal$^{3}$Man$_3$ is difficult using the standard gradient procedure. However, a differentiation is possible based on the measurement using MS or by applying a second elution gradient.

GlcMOS and GalMOS concentrations were determined using $^{1}$H NMR, and stock solutions were prepared to establish calibration curves. RRF (Table 1) were determined using the internal standard compound IMT, allowing for a semi-quantitative analysis of the (hetero)mannan structural units without the need for recalibration.

Correlation coefficients >0.99 for all calibration curves indicate good linearity (Table S 10). The process coefficients of variation for the GlcMOS and GalMOS calibration curves were <7%, demonstrating high reproducibility within the concentration range investigated. The calibration curves of the MOS also showed acceptable values with process coefficients of variation <11%. The slightly worse precision data for MOS can be attributed to the extended calibration range of 0.1–24 μM and 0.25–24 μM, respectively, compared to the calibration range of GlcMOS and GalMOS of 0.1–12 μM (Table 1). This larger concentration range was chosen because mannobiose and mannotriose are often the dominant oligosaccharides in the analyzed samples. By expanding the calibration range, all analytes can be detected in a single run. As often the case for PAD detection, a quadratic fit of the calibration curve might be better suitable then a linear fit explaining the slightly worse precision data for MOS as compared to GlcMOS and GalMOS; however, using a quadratic fit would not allow the usage of standardized RRF. Table 1 shows relevant application and statistical data of the profiling approach including LOD and LOQ. In addition to the relative retention times (RRT) used for identification purposes, Table 1 also shows *m/z* data for MS based identification if needed.

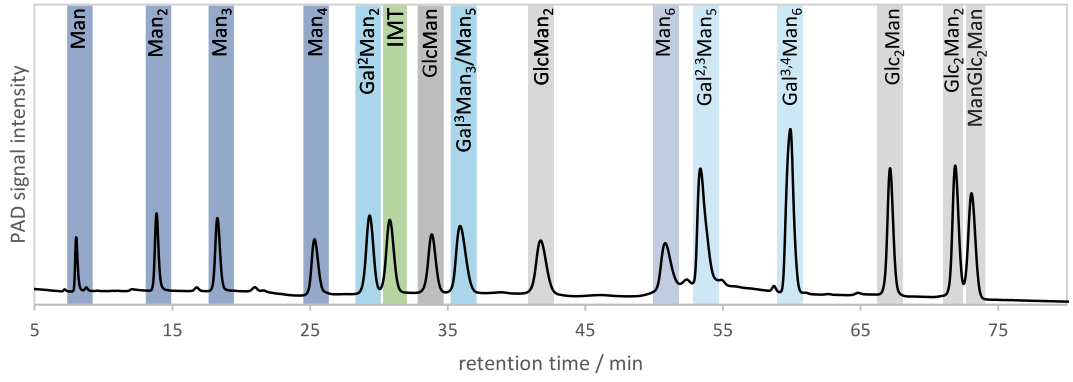


**Fig. 3.** Chromatogram of manno-, glucomanno- and galactomannooligosaccharides and isomaltotriose (IMT) as internal standard compound, which were separated using the developed profiling approach measured by high-performance anion-exchange chromatography with pulsed amperometric detection (PAD). Nomenclature is explained in Fig. 2. Man: mannose, Man$_2$: mannobiose, Man$_3$: mannotriose, Man$_4$: mannotetraose, Man$_5$: mannopentaose, Man$_6$: mannohexaose.

**Table 1**
Overview of application and statistical data for the analysis of manno-, glucomanno- and galactomannooligosaccharides: relative retention times (RRT), relative response factors (RRF), mass to charge ratios (*m/z*), quasimolecular ions, molecular weights, calibration ranges, limits of detection (LOD), and limits of quantification (LOQ). The nomenclature is explained in Fig. 2. Man: mannose, $Man_2$: mannobiose, $Man_3$: mannotriose, $Man_4$: mannotetraose, $Man_5$: mannopentaose, $Man_6$: mannohexaose.

| Analyte | RRT | RRF | *m/z* | Quasimolecular ion | Molecular weight/g/mol | Calibration range/µM | LOD/µM | LOQ/µM |
|---|---|---|---|---|---|---|---|---|
| Man | 0.260 | 2.930 | 187 | $[M + Li]^+$ | 180 | 0.25–24 | 0.100 | 0.250 |
| $Man_2$ | 0.448 | 1.370 | 349 | $[M + Li]^+$ | 342 | 0.10–24 | 0.010 | 0.025 |
| $Man_3$ | 0.590 | 1.170 | 511 | $[M + Li]^+$ | 504 | 0.10–24 | 0.050 | 0.100 |
| $Man_4$ | 0.816 | 1.080 | 673 | $[M + Li]^+$ | 666 | 0.25–24 | 0.050 | 0.250 |
| $Gal^2Man_2$ | 0.951 | 0.660 | 511 | $[M + Li]^+$ | 504 | 0.10–12 | 0.025 | 0.050 |
| GlcMan | 1.100 | 0.791 | 349 | $[M + Li]^+$ | 342 | 0.10–12 | 0.050 | 0.100 |
| $Man_5$ | 1.160 | 1.050 | 421 | $[M + 2•Li]^{2+}$ | 828 | 0.25–24 | 0.050 | 0.250 |
| $Gal^3Man_3$ | 1.170 | 0.582 | 673 | $[M + Li]^+$ | 666 | 0.10–12 | 0.025 | 0.050 |
| $GlcMan_2$ | 1.360 | 0.648 | 511 | $[M + Li]^+$ | 504 | 0.10–12 | 0.050 | 0.100 |
| $Man_6$ | 1.650 | 0.846 | 502 | $[M + 2•Li]^{2+}$ | 990 | 0.25–24 | 0.100 | 0.250 |
| $Gal^{2,3}Man_5$ | 1.730 | 0.375 | 583 | $[M + 2•Li]^{2+}$ | 1152 | 0.10–12 | 0.010 | 0.025 |
| $Gal^{3,4}Man_6$ | 1.940 | 0.307 | 664 | $[M + 2•Li]^{2+}$ | 1314 | 0.10–12 | 0.010 | 0.025 |
| $Glc_2Man$ | 2.180 | 0.463 | 511 | $[M + Li]^+$ | 504 | 0.10–12 | 0.025 | 0.050 |
| $Glc_2Man_2$ | 2.330 | 0.419 | 673 | $[M + Li]^+$ | 666 | 0.10–12 | 0.025 | 0.050 |
| $ManGlc_2Man$ | 2.370 | 0.461 | 673 | $[M + Li]^+$ | 666 | 0.10–12 | 0.025 | 0.050 |

#### 3.2.2. Limitations of the approach

To evaluate whether the captured oligosaccharides of the profiling approach represent the analyzed (hetero)mannans, the profiling results were compared with the monosaccharide compositions of KM and LBG. The comparison is feasible for these two materials as they consist predominantly of (hetero)mannans and contain only minor amounts of other polysaccharides that could otherwise interfere with the results. The proportion of Glc and the degree of Gal substitution of the (hetero) mannans can be calculated from the determined molar composition of MOS, GlcMOS, and GalMOS. According to this calculation, the proportion of Glc in the glucomannans of KM is approximately 22%. The monosaccharide composition showed a Man proportion of 63 mol% and a Glc proportion of 37 mol% for KM (Man:Glc ≈ 1.7:1), which is comparable to the Man:Glc ratio of 1.6:1 for KM glucomannans in the literature (Maeda et al., 1980). Similarly, the degree of Gal substitution was calculated for LBG based on the profiling results. A value of approximately 10% was obtained for LBG. However, based on the molar proportions of Gal and Man in the monosaccharide composition, this value is approximately 33% for LBG. Literature suggests a degree of substitution of LBG galactomannans of around 25% (Moreira & Filho, 2008).

These data show a deviation of the Man:Glc and Man:Gal ratios of heteromannans calculated by using either the profiling approach or the monosaccharide composition. Application of the profiling approach captures only regions of the (hetero)mannans that are cleaved into oligosaccharides by the mannanase. In addition, if oligosaccharides were released that are structurally different from the standard compounds used these would not be identified and, thus, not included into the calculation. By comparing the different ratios it was assumed that both the KM glucomannans and the LBG galactomannans contain sections that have a particularly high proportion of Glc or Gal, respectively. These regions cannot sufficiently be hydrolyzed by the used mannanase, resulting in oligo- or even polysaccharides that are not detected by the HPAEC-PAD profiling approach.

To verify this hypothesis, the samples after mannanase treatment were separated into two fractions using HPSEC-RI (Fig. S 3). In this way, a low molecular weight fraction was obtained containing the majority of the oligosaccharides detected in the profiling approach. The second fraction contained compounds of larger molecular weight. The monosaccharide composition of the larger molecular weight fraction demonstrated a Glc content of 52%, whereas the low molecular weight fraction showed a Glc content of 37%. Therefore, the insufficiently cleaved regions of the glucomannans are particularly rich in Glc. A comparable observation was made for the LBG galactomannans. Here, the fraction that is not detected by the profiling approach had a Gal substitution degree of 45%. In contrast, the substitution degree of the fraction that contain the detected oligosaccharides was only 21%. Based on these data, the assumption that highly substituted clusters in galactomannans of LBG and longer Glc-containing stretches in glucomannans of KM exist can be confirmed (Daas et al., 2000). However, it should also be noted that mannans are able to partially form crystalline areas, which confer resistance to mechanical treatment (Buckeridge et al., 2000; Millane & Hendrixson, 1994) and cannot be cleaved by mannanases, too.

Nevertheless, the developed profiling approach enables the specific detection of MOS, GlcMOS, and GalMOS and, thus the classification as homomannan, glucomannan, or galactomannan. This classification can also be clearly applied to mixtures of polysaccharides, e.g. if glucomannans are analyzed in the presence of cellulose or xyloglucans. The existence of galactoglucomannans can only be inferred indirectly from the simultaneous occurrence of GlcMOS and GalMOS; however, the possibility that two populations of heteromannans, that is, glucomannans and galactomannans, exist in the same sample cannot be excluded. Thus, a next step in the development of profiling approaches should be a screening approach regarding galactoglucomannans, which, however, requires standard compounds of galactoglucomannooligosaccharides (GalGlcMOS).

### 3.3. Application

#### 3.3.1. Screening of konjac meal and locust bean gum

To compare the mannan structure of different samples of the principally same plant material (botanical source), four KM and four LBG samples (each includes the material used for standard isolation, KM 1 and LBG 1) were analyzed by using the profiling approach. All five isolated GlcMOS were detected in all four KM samples (Fig. 4a). Furthermore, unsubstituted MOS up to a DP of 4 were detected, with mannobiose constituting the largest proportion in all four KM samples. Among the GlcMOS, GlcMan and $GlcMan_2$ predominated. However, GlcMOS with a higher glucose content ($Glc_2Man$, $Glc_2Man_2$, and $ManGlc_2Man$) were also detected. Overall, there were hardly any differences between the four different KM samples. It can therefore be assumed that the glucomannan contained in KM exhibits a similar structure regardless of the origin and processing of the KM. However, it cannot be ruled out that the products, although obtained from different suppliers, may originate from the same production.

Analysis of the four LBG samples revealed similar distributions for three of them (Fig. 4b). Mannobiose predominated in all LBG samples. In LBG 1–3, mannobiose was followed by mannotriose, whereas large amounts of monomeric mannose were detected in LBG 4. LBG 4 showed

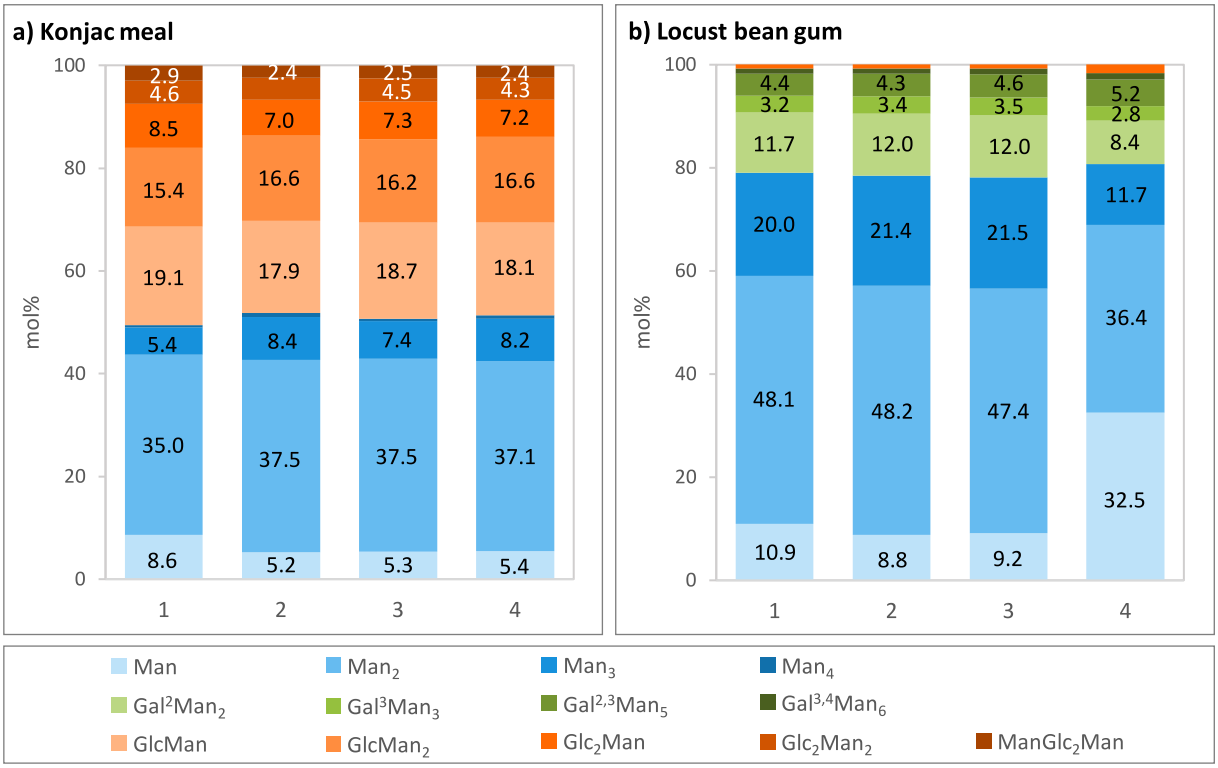


**Fig. 4.** Molar composition of manno-, glucomanno- and galactomannooligosaccharides after enzymatic hydrolysis using *endo*-β-1,4-mannanase of four samples of konjac meal (KM) and four samples of locust bean gum (LBG, in mol%, $n = 2$). KM 1 and LBG 1 are the materials used for isolation of standard compounds. The nomenclature is explained in Fig. 2. Man: mannose, $Man_2$: mannobiose, $Man_3$: mannotriose, $Man_4$: mannotetraose, $Man_5$: mannopentaose, $Man_6$: Mannohexaose.

also deviations in the proportions of the other oligosaccharides compared to LBG 1–3. Nevertheless, all isolated GalMOS were detected in all LBG samples, with $Gal_2Man_2$ exhibiting the highest proportion. The varying GalMOS and MOS profiles were also reflected in the monosaccharide composition after methanolysis. The dominant monosaccharide of LBG 4 was arabinose (35.5 mol%) instead of mannose, which dominated in the other LBG samples (approximately 73 mol%). Therefore, this product sold as LBG not only consists of galactomannans, but presumably also contains a significant amount of pectin (particularly arabinans). Additionally, it can be hypothesized that the high proportion of mannose in the distribution as determined by the profiling approach was (at least partially) released during manufacturing of LBG 4 and not during the analysis performed here. LBG can be obtained from carob seeds using various methods (e.g., acid or heat treatment), which affect the captured carbohydrates (Petitjean & Isasi, 2022). However, similar galactomannan structures were clearly demonstrated for LBG 1–3.

### 3.3.2. *Screening of different plant samples*

Finally, the developed HPAEC-PAD screening approach was applied to various plant samples, for which literature indicated the presence of mannans. Different mannose-containing structural units were successfully detected in coffee, coconut, and blackcurrant samples (Fig. 5). Data for additional plant samples are shown in Fig. S 4.

In all plant samples, large proportions of mannobiose (usually around 50 mol%) and mannotriose (around 30 mol%) were released enzymatically, which can presumably be attributed to the cleavage mechanism of the mannanase used. When comparing the mannans from IDF and SDF, larger proportions of GlcMOS and GalMOS were released from SDF than from IDF. Thus, the mannans from SDF have a higher proportion of Glc and/or Gal and are therefore more soluble than homomannans. Since other Glc- and or Gal-containing polysaccharides besides heteromannans are present in the plant samples, it was not possible to calculate the proportion of Glc in glucomannans and the degree of Gal substitution in galactomannans based on the monosaccharide composition.

The polysaccharides of raw coffee beans contained 52.6 mol% Man in the IDF fraction and 22.7 mol% Man in the SDF fraction, confirming the predominance of mannans in raw coffee beans (Redgwell et al., 2003). Using the developed profiling approach, small proportions of GalMOS were detected besides high molar proportions of mannobiose and mannotriose in the IDF and SDF of raw coffee beans, predominantly $Gal^2Man_2$ and $Gal^3Man_3$. Larger GalMOS ($Gal^{2,3}Man_5$ and $Gal^{3,4}Man_6$) were also detected in SDF. In IDF, these oligosaccharides were observed, but below the LOQ. In addition to GalMOS, GlcMan was detected in IDF and SDF, whereas $GlcMan_2$ and $Glc_2Man$ were also detected in SDF. Thus, IDF and SDF of raw coffee beans consist predominantly of galactomannans with small proportions of gluco- and/or galactoglucomannans. Higher substituted galactomannans have been described as being easier to extract (Redgwell et al., 2003) in accordance with our data: SDF (6.5 mol%) contains a higher proportion of hetero-MOS than IDF (2.4 mol%). Roasted coffee beans exhibit the same hetero-MOS as raw coffee beans, but in lower quantities, suggesting a favored degradation of branched structures. In some cases, their concentrations were below the LOQ and therefore could not be quantified. In the literature, the application of methylation analysis of high molecular weight material of raw and roasted coffee beans also showed a slightly lower proportion of 1,4,6-linked mannopyranose compared to the total number of binding types of Man for samples from roasted coffee beans. This structural change was likely caused by the roasting process (Nunes & Coimbra, 2001).

Copra meal is highly enriched in mannans (Man in IDF: 82.6 mol%; in SDF: 29.8 mol%). Using the profiling approach, mannobiose was detected as the dominant hydrolysis product, followed by mannotriose and Man, as previously described (Ghosh et al., 2015). It has also been suggested that GalMOS or GlcMOS are present in small quantities. However, these have not yet been unambiguously identified (Cuong

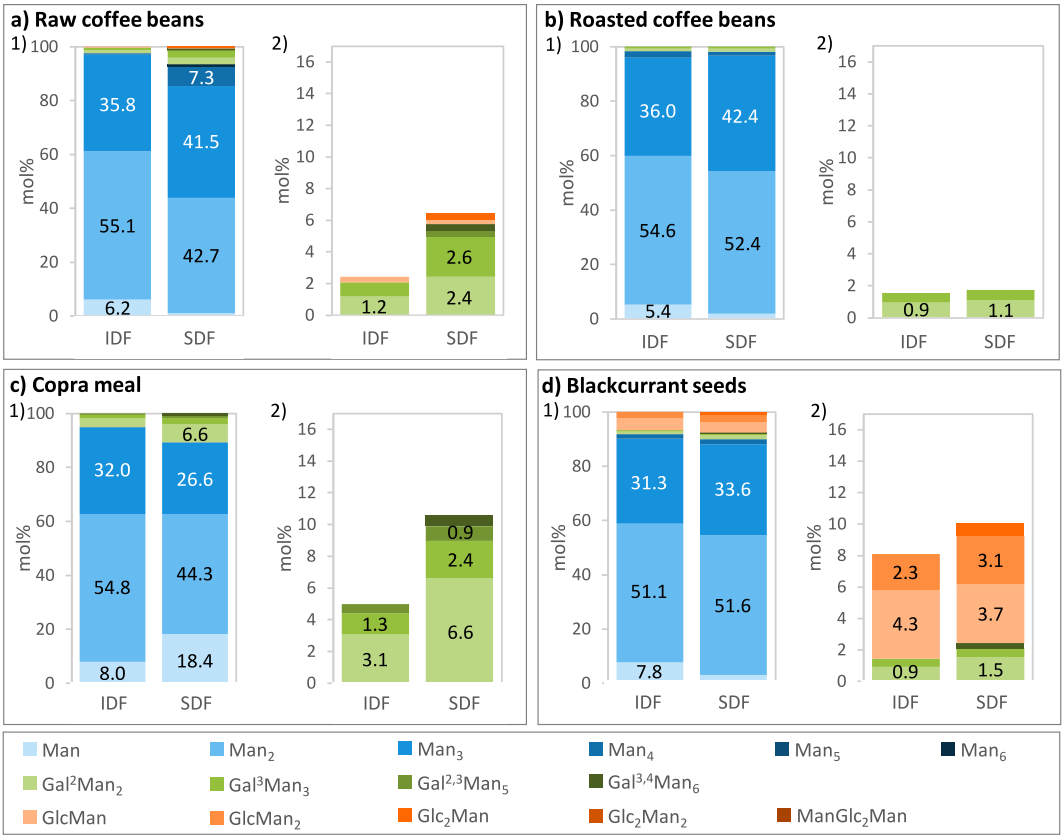


**Fig. 5.** Molar composition of manno-, glucomanno- and galactomannooligosaccharides after enzymatic hydrolysis of insoluble (IDF) and soluble fiber (SDF) from various plant samples using *endo*-β-1,4-mannanase (in mol%, $n = 2$). Graphs on the left (1) show the total composition and graphs on the right (2) show - enlarged - the composition of the proportions of heteromannooligosaccharides only. The nomenclature is explained in Fig. 2. Man: mannose, $Man_2$: mannobiose, $Man_3$: mannotriose, $Man_4$: mannotetraose, $Man_5$: mannopentaose, $Man_6$: Mannohexaose.

et al., 2024). Application of the profiling approach to copra meal IDF detected $Gal^2Man_2$, $Gal^3Man_3$, and $Gal^{2,3}Man_5$ in decreasing molar proportions, demonstrating the presence of galactomannans. Also, $Gal^{3,4}Man_6$ as well as GlcMan, and $GlcMan_2$ were determined, but below the LOQ. The same hetero-MOS as in IDF were detected in SDF, but in larger portions. The detection of $Gal^{2,3}Man_5$ and $Gal^{3,4}Man_6$ demonstrated areas with two adjacent mannose units that carry galactose side-chains in copra meal galactomannans. According to the results of the profiling approach and in accordance with literature, the polysaccharides in copra meal are primarily homomannans and, in smaller quantities, galactomannans and galactoglucomannans or glucomannans (Saittagaroon et al., 1983).

IDF of blackcurrant seeds are also rich in mannans (Man: 66.2 mol %). The polysaccharides of SDF have an average Man content of 30.9 mol%. All hetero-MOS in the profiling approach were detected, but in some cases only qualitatively. GlcMOS with one Glc unit accounted for the largest share. The molar composition of the oligosaccharides of SDF of blackcurrant seeds is comparable but the overall proportion of hetero-MOS is larger (10.1 mol% in SDF vs. 8.1 mol% in IDF). To date, there are no specific statements in the literature regarding the occurrence of heteromannans in blackcurrants or currants in general (Hilz et al., 2005; Steck et al., 2025). Here, the profiling approach has shown that, besides dominant homomannans, glucomannans are major components, with galactomannans (or glucogalactomannans) being present in smaller quantities.

## 4. Conclusion

This study demonstrates a multistep isolation process to generate GlcMOS and GalMOS as standard compounds (nine in total) for the development of a profiling approach for the structural analysis of (hetero)mannans by HPAEC-PAD. The developed profiling approach is suitable for releasing MOS, GlcMOS, and GalMOS from plant materials, which are unambiguously identified and semi-quantitatively determined using HPAEC-PAD, optionally in combination with MS. Although this approach is very well suited to categorize (hetero)mannans according to their building blocks, interpretation of the data needs to consider that only enzymatically accessible regions of the (hetero) mannans are captured. To demonstrate the suitability of the approach to real plant-based samples, coffee beans, copra meal, and blackcurrant seeds were analyzed, clearly confirming the occurrence of galactomannans and/or glucomannans.

## CRediT authorship contribution statement

**Lisa Johanna Wagner:** Writing – original draft, Visualization, Methodology, Investigation, Formal analysis, Data curation, Conceptualization. **Mirko Bunzel:** Writing – review & editing, Supervision, Resources, Methodology, Conceptualization.

## Declaration of competing interest

The authors declare the following financial interests/personal relationships which may be considered as potential competing interests: Lisa Wagner reports financial support was provided by Stifterverband für die Deutsche Wissenschaft e.V. If there are other authors, they declare that they have no known competing financial interests or personal relationships that could have appeared to influence the work reported in this paper.

## Acknowledgements

We thank the Stifterverband für die Deutsche Wissenschaft e.V. for partial funding of this project.

## Appendix A. Supplementary data

Supplementary data to this article can be found online at https://doi.org/10.1016/j.carbpol.2026.125496.

## Data availability

Data will be made available on request.

## References

Albersheim, P., Devins, D. J., English, P. D., & Karr, A. (1967). A method for the analysis of sugar in plant cell-wall polysaccharides by gas-liquid chromatography. *Carbohydrate Research, 5*, 340–345.

Bubb, W. A. (2003). NMR spectroscopy in the study of carbohydrates: Characterizing the structural complexity. *Concepts in Magnetic Resonance Part A, 19A*, 1–19. https://doi.org/10.1002/cmr.a.10080

Buckeridge, M. S., Dietrich, S. M. C., & De Lima, D. U. (2000). Galactomannans as the reserve carbohydrate in legume seeds. *Carbohydrate Reserves in Plants - Synthesis and Regulation, 26*, 283–316. https://doi.org/10.1016/S0378-519X(00)80015-X

Bunzel, M., Ralph, J., Marita, J. M., Hatfield, R. D., & Steinhart, H. (2001). Diferulates as structural components in soluble and insoluble cereal dietary fibre. *Journal of the Science of Food and Agriculture, 81*, 653–660. https://doi.org/10.1002/jsfa.861

Cataldi, T. R. I., Campa, C., & De Benedetto, G. E. (2000). Carbohydrate analysis by high-performance anion-exchange chromatography with pulsed amperometric detection: The potential is still growing. *Fresenius Journal of Analytical Chemistry, 368*, 739–758. https://doi.org/10.1007/s002160000588

Cescutti, P., Campa, C., Delben, F., & Rizzo, R. (2002). Structure of the oligomers obtained by enzymatic hydrolysis of the glucomannan produced by the plant *Amorphophallus konjac*. *Carbohydrate Research, 337*, 2505–2511. https://doi.org/10.1016/s0008-6215(02)00332-4

Corradini, C., Cavazza, A., & Bignardi, C. (2012). High-performance anion-exchange chromatography coupled with pulsed electrochemical detection as a powerful tool to evaluate carbohydrates of food interest: Principles and applications. *International Journal of Carbohydrate Chemistry, 1*, 1–13. https://doi.org/10.1155/2012/487564

Cuong, N. C., Haltrich, D., Min, T. T., Nguyen, T. H., & Yamabhai, M. (2024). Value creation of copra meal mannan into functional manno-oligosaccharides (β-MOS) using the mannanase *Bacillus* man B (*Bl*Man26B). *Scientific Reports, 14*, 22363. https://doi.org/10.1038/s41598-024-73255-5

Daas, P. J. H., Schols, H. A., & De Jongh, H. H. J. (2000). On the galactosyl distribution of commercial galactomannans. *Carbohydrate Research, 329*, 609–619. https://doi.org/10.1016/S0008-6215(00)00209-3

De Ruiter, G. A., Schols, H. S., Voragen, A. G. J., & Rombouts, F. M. (1992). Carbohydrate analysis of water-soluble uranic acid-containing polysaccharides with high-performance anion-exchange chromatography using methanolysis combined with tfa hydrolysis is superior to four other methods. *Analytical Biochemistry, 207*, 176–185. https://doi.org/10.1016/0003-2697(92)90520-H

Duus, J. O., Gotfredsen, C. H., & Bock, K. (2000). Carbohydrate structural determination by NMR spectroscopy: Modern methods and limitations. *Chemical Reviews, 100*, 4589–4614. https://doi.org/10.1021/cr990302n

Ghosh, A., Verma, A. K., Tingirikari, J. R., Shukla, R., & Goyal, A. (2015). Recovery and purification of oligosaccharides from copra meal by recombinant *endo*-β-mannanase and deciphering molecular mechanism involved and its role as potent therapeutic agent. *Molecular Biotechnology, 57*, 111–127. https://doi.org/10.1007/s12033-014-9807-4

Gniechwitz, D., Brueckel, B., Reichardt, N., Blaut, M., Steinhart, H., & Bunzel, M. (2007). Coffee dietary fiber contents and structural characteristics as influenced by coffee type and technological and brewing procedures. *Journal of Agricultural and Food Chemistry, 55*, 11027–11034. https://doi.org/10.1021/jf072389g

Hilz, H., Bakx, E. J., Schols, H. A., & Voragen, A. G. J. (2005). Cell wall polysaccharides in black currants and bilberries - characterisation in berries, juice, and press cake. *Carbohydrate Polymers, 59*, 477–488. https://doi.org/10.1016/j.carbpol.2004.11.002

Karplus, M. (1959). Contact electron-spin coupling of nuclear magnetic moments. *Journal of Chemical Physics, 30*, 11–15. https://doi.org/10.1063/1.1729860

Lee, Y. C. (1990). High-performance anion-exchange chromatography for carbohydrate analysis. *Analytical Biochemistry, 189*, 151–162. https://doi.org/10.1016/0003-2697(90)90099-u

Maeda, M., Shimahara, H., & Sugiyama, N. (1980). Detailed examination of the branched structure of konjac glucomannan. *Agricultural and Biological Chemistry, 44*, 245–252. https://doi.org/10.1271/bbb1961.44.245

Mccleary, B. V., & Matheson, N. K. (1983). Action patterns and substrate-binding requirements of beta-D-mannanase with mannosaccharides and mannan-type polysaccharides. *Carbohydrate Research, 119*, 191–219. https://doi.org/10.1016/0008-6215(83)84056-7

Melton, L. D., Smith, B. G., Ibrahim, R., & Schröder, R. (2009). Mannans in primary and secondary plant cell walls. *New Zealand Journal of Forestry Science, 39*, 153–160.

Mikkelson, A., Maaheimo, H., & Hakala, T. K. (2013). Hydrolysis of konjac glucomannan by *Trichoderma reesei* mannanase and endoglucanases Cel7B and Cel5A for the production of glucomannooligosaccharides. *Carbohydrate Research, 372*, 60–68. https://doi.org/10.1016/j.carres.2013.02.012

Millane, R. P., & Hendrixson, T. L. (1994). Crystal structures of mannan and glucomannans. *Carbohydrate Polymers, 25*, 245–251. https://doi.org/10.1016/0144-8617(94)90050-7

Moreira, L. R. S., & Filho, E. X. F. (2008). An overview of mannan structure and mannan-degrading enzyme systems. *Applied Microbiology and Biotechnology, 79*, 165–178. https://doi.org/10.1007/s00253-008-1423-4

Nunes, F. M., & Coimbra, M. A. (2001). Chemical characterization of the high molecular weight material extracted with hot water from green and roasted arabica coffee. *Journal of Agricultural and Food Chemistry, 49*, 1773–1782. https://doi.org/10.1021/jf0012953

Petitjean, M., & Isasi, J. R. (2022). Locust bean gum, a vegetable hydrocolloid with industrial and biopharmaceutical applications. *Molecules, 27*, 8265. https://doi.org/10.3390/molecules27238265

Pettolino, F. A., Walsh, C., Fincher, G. B., & Bacic, A. (2012). Determining the polysaccharide composition of plant cell walls. *Nature Protocols, 7*, 1590–1607. https://doi.org/10.1038/nprot.2012.081

Prajapati, V. D., Jani, G. K., Moradiya, N. G., Randeria, N. P., Nagar, B. J., Naikwadi, N. N., & Variya, B. C. (2013). Galactomannan: A versatile biodegradable seed polysaccharide. *International Journal of Biological Macromolecules, 60*, 83–92. https://doi.org/10.1016/j.ijbiomac.2013.05.017

Redgwell, R. J., Curti, D., Rogers, J., Nicolas, P., & Fischer, M. (2003). Changes to the galactose/mannose ratio in galactomannans during coffee bean (*Coffea arabica* L.) development: Implications for *in vivo* modification of galactomannan synthesis. *Planta, 217*, 316–326. https://doi.org/10.1007/s00425-003-1003-x

Saeman, J. F., Bubl, J. L., & Harris, E. E. (1945). Quantitative saccharification of wood and cellulose. *Industrial and Engineering Chemistry-Analytical Edition, 17*, 35–37. https://doi.org/10.1021/i560137a008

Saittagaroon, S., Kawakishi, S., & Namiki, M. (1983). Characterization of polysaccharides of copra meal. *Journal of the Science of Food and Agriculture, 34*, 855–860. https://doi.org/10.1002/jsfa.2740340813

Salo, M.-L., & Suomi, K. (1972). Carbohydrate and acid composition of finnish berries. *Agricultural and Food Science, 44*, 68–75. https://doi.org/10.23986/afsci.71812

Sassaki, G. L., Gorin, P.a. J., Souza, L. M., Czelusniak, P. A., & Iacomini, M. (2005). Rapid synthesis of partially O-methylated alditol acetate standards for GC-MS: Some relative activities of hydroxyl groups of methyl glycopyranosides on Purdie methylation. *Carbohydrate Research, 340*, 731–739. https://doi.org/10.1016/j.carres.2005.01.020

Singh, S., Singh, G., & Arya, S. K. (2018). Mannans: An overview of properties and application in food products. *International Journal of Biological Macromolecules, 119*, 79–95. https://doi.org/10.1016/j.ijbiomac.2018.07.130

Steck, J., Eichhöfer, H., & Bunzel, M. (2025). Comprehensive characterization of the polysaccharide composition and xyloglucan architecture of four berry fruits and their macroscopic fruit components. *Journal of Agricultural and Food Chemistry, 73*, 10545–10558. https://doi.org/10.1021/acs.jafc.4c11864

Steck, J., Kaufhold, L., & Bunzel, M. (2021). Structural profiling of xyloglucans from food plants by high-performance anion-exchange chromatography with parallel pulsed amperometric and mass spectrometric detection. *Journal of Agricultural and Food Chemistry, 69*, 8838–8849. https://doi.org/10.1021/acs.jafc.1c02967

Van Zyl, W. H., Rose, S. H., Trollope, K., & Görgens, J. F. (2010). Fungal β-mannanases: Mannan hydrolysis, heterologous production and biotechnological applications. *Process Biochemistry, 45*, 1203–1213. https://doi.org/10.1016/j.procbio.2010.05.011

Wefers, D., & Bunzel, M. (2016). Arabinan and galactan oligosaccharide profiling by high performance anion-exchange chromatography with pulsed amperometric detection (HPAEC-PAD). *Journal of Agricultural and Food Chemistry, 64*, 4656–4664. https://doi.org/10.1021/acs.jafc.6b01121

Yao-Ling, L., Rong-Hua, D., Ni, C., Juan, P., & Jie, P. (2013). Review of konjac glucomannan: Isolation, structure, chain conformation and bioactivities. *Journal of Single Molecule Research, 1*, 7–14. https://doi.org/10.12966/jsmr.07.03.2013